Photographic Study of the Transition Between the Quasi-Detonation and Choking Regimes

D. H.B. Lieberman, J. H.S. Lee
McGill University
Montreal, Quebec, Canada
E-mail: daniell@caltech.edu

Introduction

The purpose of the current work is to investigate the transition of combustion waves propagating in an obstacle filled tube from the quasi-detonation regime to the choking regime. Quasi-detonations are characterized by detonation velocities in the range of V_{cj} to about $0.65V_{cj}$. In the choking regime, combustion waves propagate at approximately the sound speed of the burnt products ($0.5V_{cj}$). It is found (1) that in a tube with orifice plate obstacles there is a sharp transition between the quasi-detonation and choking regime, corresponding to an abrupt drop in detonation velocity. However, experiments in different obstacle geometries (2) for example packed beds indicate that the transition is more gradual and in some cases it is just an inflection.

Although quasi-detonations and choking combustion waves have been well documented (3-4) very little work has been done on the behavior of the transition region between them. Studying detonations in this region can illustrate the change in propagation mechanisms between the choking and quasi-detonation regimes. Thus, the present work will investigate the phenomenon of the combustion wave in the transition region. Obstacle spacing, geometry and blockage ratio will be varied along with mixture sensitivity and composition. In an effort to elucidate the transient behavior of the combustion wave in the transition regime streak photography is used to observe the propagation of the combustion waves under the various initial and boundary conditions.

Experimental Setup

The experiments are carried out in a 4m long acrylic tube with a 50.8mm inside diameter. Figure 1 is a schematic of the experimental facility. The mixtures used in the experiments are stoichiometric oxy-acetylene with 0%, 50% and 75% Argon dilution prepared in a mixed tank by method of partial pressure. Prior to each test the tube is evacuated to pressures better than 100Pa. The combustible mixture is then inserted into the tube facility to a pressure at least 150% of the desired initial pressure before it is lowered back down. A detonation is initiated in the smooth section of the tube via a high voltage spark or a driver section. The detonation travels through the smooth section of the tube to ensure a stable C-J detonation and then enters the obstacle section. Streak photographs are taken of the detonation as it passes from the smooth to the obstacle section. The camera operates with a rotating drum and is of Russian design. Optic probes also line the tube to get a measure of the detonations mean velocity. The obstacle section consists of orifice plates with blockage ratios of Br = 0.45 and 0.55. They are spaced at ¼d, ½d and 1d intervals to form an obstacle section of 0.9m in length. d refers to the inner tube diameter.

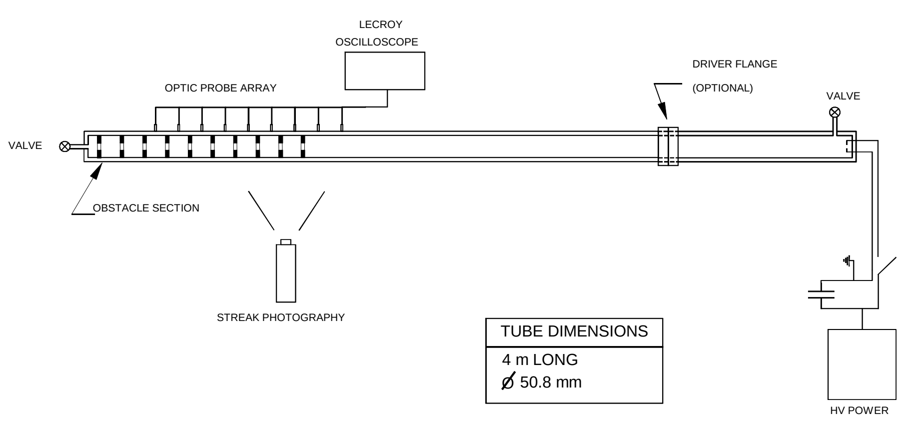

Figure 1: Experimental Facility

Results and discussion

Fig 2a-e shows streak photographs of quasi-detonations under various obstacle configurations and argon dilutions. A smooth line representing a C-J detonation is visible just before the leading obstacle. As the C-J detonation enters the obstacle section a shock wave is reflected back toward the ignition source. The curve in the reflected shock is a result of the shockwave moving into an expanded flow from the closed ended boundary condition. As the detonation propagates into the obstacle section it takes less than 1 tube diameter to reach its quasi-detonation velocity. Regardless of the obstacle configuration or amount of Argon dilution, all the quasi-detonations are steady over the obstacle set. Slight variations in quasi-detonation velocity occur in between obstacle pairs. Fig 2a-e show that after each obstacle there is a velocity decay followed by an abrupt acceleration. Work carried out by Theodorczyk (5) showed that quasi-detonations propagate via a failure by diffraction followed by re-initiation from shock-boundary interaction. The luminosity is almost constant for quasi-detonations over multiple obstacles. This indicates a regularity in heat release through a set of obstacles. Fig 2e is a streak photograph of a quasi-detonation from a 75%Ar mixture. The quasi-detonation is steady over multiple obstacles, however, there are fluctuations on the order of 1-2 obstacles. As well, the luminosity has some fluctuations through the obstacle section. The differences between fig 2a-d and 2e are attributed to the effects of Argon dilution. The addition of Argon changes the dominant failure mechanisms. For irregular mixtures detonation failure by diffraction off obstacles occurs if all the cells are cooled sufficiently. For high Argon dilution (regular cells) failure arises from excess curvature of the detonation front. The details of these mechanisms are summarized in a review paper by Lee (6).

Fig 3a-e shows streak photographs of combustion waves in the choking regime under various obstacle arrangements and argon dilution. A C-J detonation is attained prior to entering the obstacle section. All the images show that the combustion wave has a steady velocity across the obstacle section. The velocity of choking regime combustion waves is approximately $0.5V_{cj}$. The streak photographs show that the quasi-detonation and choking regime combustion waves behave differently between obstacles. The choking regime combustion waves all generate bright spots in between a pair of obstacles. The appearance of this bright spot depends on the obstacle geometry. Fig 3a,b shows that the bright spots arise 5-10micro seconds after the leading edge of the combustion wave. Fig 3c shows that for 1D spacing the bright spots are less defined and occur with little or no delay from the reaction leading edge. Fig 3d,e show streak photographs of mixtures with Argon dilution. The addition of 50%Ar does not change the behavior of the combustion wave between obstacles from the 0%Ar case. However, the addition of 75%Ar results in a very regular pattern of bright spots occurring at the front of the combustion wave. Consequently, there is very little luminosity other than these bright spots.

Fig 4a-e are streak photographs taken in the transition region between the quasi-detonation and choking regimes. As the detonation enters the obstacles its velocity begins to fluctuate. The magnitude of the oscillations is dependent on the obstacle spacing (fig 4a-c). The combustion waves in the transition region highlight features from both quasi-detonation and choking regime combustion waves. The luminosity varies as the detonation accelerates and slows down. The start of an oscillation is accompanied by a bright spot and an acceleration. The detonation then gently decays over a number of obstacles and the cycle repeats itself. For 1/4D and 1/2D spacings the oscillations have 2 characteristic wavelengths of $P/\lambda \approx 11$-12 and $P/\lambda \approx 23$-24 where P is the length of an oscillation measured along the tube. The oscillations are less pronounced at 1D spacing (fig 4c). However, they tend to oscillate at the same P/λ values as the other spacings. The variation of blockage ratio or the addition of 50%Ar does not change the behavior of the transition region. However, by adding 75%Ar the large oscillations do not arise. Instead smaller fluctuations in velocity on the order of 1-2 obstacles are present. The absence of oscillations in the 75%Ar dilution case suggests that the failing mechanisms for quasi-detonations depend on mixture composition. Similar to the critical tube diameter problem investigated by Desbordes (7).

%Ar Br Spacing	λ_{crit} (mm)	L/λ
0%Ar Br = 0.45 ¼d	6	2.12
½d	8.5	2.98
1d	23	2.2
Br = 0.55 ¼d	5.2	2.44
½d	9	2.82
1d	19	2.67
50%Ar Br = 0.45 ½d	10	2.43
75%Ar Br = 0.45 ½d	5	5.08

Table 1: $C_2H_2 + 2.5O_2$ + X% Ar, Orifice

Fig 5 is a plot of the mean velocity vs. initial pressure for combustion waves through a Br = 0.55 orifice plate geometry at various spacings. The plot indicates the location of the transition in all three spacing arrangements with respect to a critical pressure. As the obstacle spacing decreases the critical pressure increases which corresponds to a decreasing cell size. Consequently, as the spacing decreases the velocity jump at the transition becomes an inflection. Table 1 highlights the L/λ

values at the transition for orifice plate geometries. L refers to the obstacle spacing. All the L/λ values are 2-3 indicating that a quasi-detonation needs at least 2 cells between a pair of obstacles to propagate. For 75%Ar dilution the L/λ value doubles similar to the double in d/λ values in the critical tube diameter problem.

Changing the obstacle geometry from orifice plates to perforated plates of the same blockage ratio (Br = 0.45) eliminates the transition and choking regime. Fig 6 shows a plot of velocity vs. initial pressure comparing perforated and orifice plates. The perforated plates remain in the quasi-detonation regime for the entire range of initial pressures tested (i.e. until the mixture sensitivity is too weak to initiate a smooth tube detonation). The absence of a choking regime and transition region indicates that the obstacle geometry plays a significant role in sustaining quasi-detonations. The large number of holes in the perforated plate allows the diffracting combustion waves to intersect and re-initiate through shock-shock shear mixing. This process maintains a higher mean velocity.

Conclusion

The results conclude that obstacle geometry controls the existence of transition. Obstacles cause the combustion wave to diffract and cool. It is therefore, the mechanisms of re-initiation that play a role in the sustaining a quasi-detonation. Orifice plate geometries give rise to a transition, however, the dominant propagation mechanisms at transition depend on mixture composition. For Argon dilutions less then 75% by volume, transition occurs as a result of a failure to re-initiate after a diffraction wave has cooled down the entire combustion wave. The oscillations in the transition regime result form an imbalance between the failure and re-initiation mechanisms. Localized explosions cause a sudden acceleration which then fails by diffraction. For Argon dilution greater then 75% transition is a result of failure to re-initiate by excessive curvature to the entire combustion front. The lack of oscillations indicates that the combustion front is less sensitive to diffractive cooling. The use of perforated plates increases the turbulent shock interactions of the mixture. Re-initiation can more readily occur resulting in a prolonged existence of quasi-detonations at lower mixture sensitivities. The absence of a choking regime requires further investigation.

Reference:

(1) Lee J. H., Knystautas R., Chan C. K., (1984) "Turbulent Flame Propagation in Obstacle-Filled Tubes", 20th Symp. On Comb., 1663-1672.

(2) Mitrofanov V. V., Lyamin G. A., Pinaev A. V., Subbotin V. A. (1991) "Propagation of Gas Explosion in Channels with Uneven Walls and in Porous Media", Dynamic Structure of Detonation in Gaseous and Dispersed Media, editor A. A. Borissov, Kluwer Academic Publishers, Netherlands, 51-75.

(3) Guenoche H., and Manson N. (1949) "Influence des Conditions aux Limites Transversals sur la Propagation des Ondes de Choc et de Combustion". Rev. Inst. Fr. Pet. 2, 53-69.

(4) Gu L. S., Knystautas R., Lee J. H. (1988) "Influence of Obstacle Spacing on the Propagation of Quasi-Detonation", Prog. Astro. Aero., 114:232-247.

(5) Teodorczyk A., Lee J. H. S., Knystautas R. (1991) "Photographic Study of the Structure and Propagation Mechanisms of Quasi-detonations in Rough Tubes", Prog. Astro. Aero., 133:223-240.

(6) Lee J.H. (1996) "On the critical diameter problem", *Dynamics of Exothermicity*, editor JR Bowen, Gordon and Breech Publishers, Netherlands, 321-336.

(7) Desbordes D., Guerraud C., Hamada L., presles H.N. (1993) "Failure of the classical dynamic parameters relationships in highly regular cellular detonation systems", *Prog. Astro. Aero.*, 153:347-359.

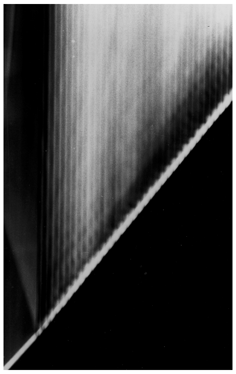

Fig 2a,
0%Ar
Br = 0.45
¼d spacing

Fig 2b,
0%Ar
Br = 0.45
½d spacing

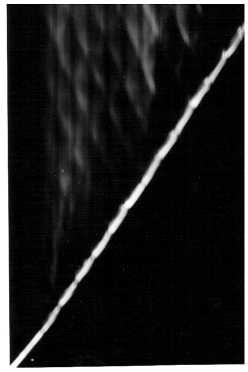

Fig 2c,
0%Ar
Br = 0.45
1d spacing

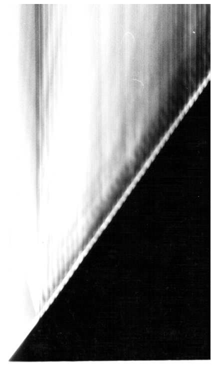

Fig 2d,
50%Ar
Br = 0.45
½d spacing

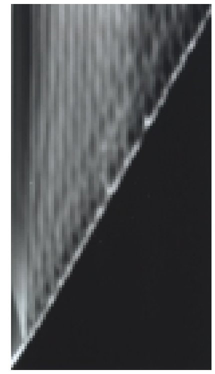

Fig 2e,
75%Ar
Br = 0.45
½d spacing

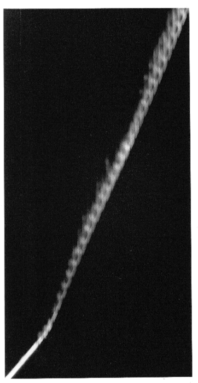

Fig 3a,
0%Ar
Br = 0.45
¼d spacing

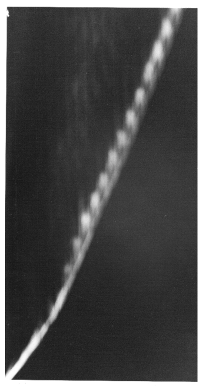

Fig 3b,
0%Ar
Br = 0.45
½d spacing

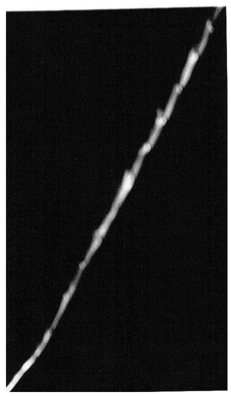

Fig 3c,
0%Ar
Br = 0.45
1d spacing

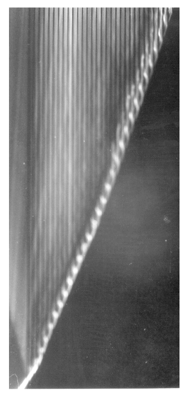

Fig 3d,
50%Ar
Br = 0.45
½d spacing

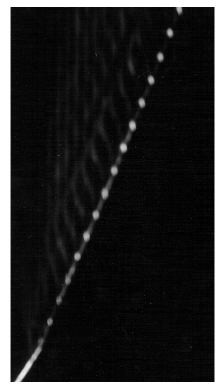

Fig 3e,
75%Ar
Br = 0.45
½d spacing

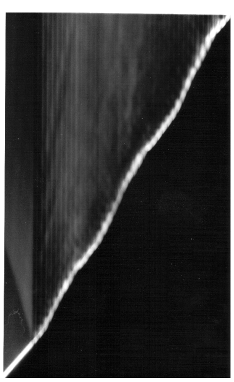

Fig 4a,
0%Ar
Br = 0.45
¼d spacing

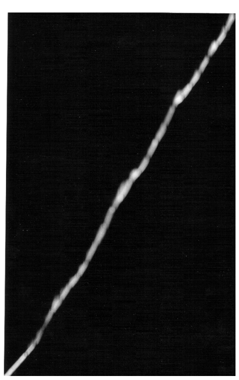

Fig 4b,
0%Ar
Br = 0.45
½d spacing

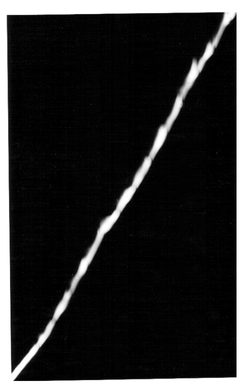

Fig 4c,
0%Ar
Br = 0.45
1d spacing

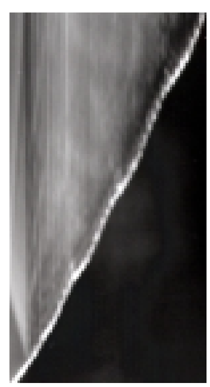

Fig 4d,
50%Ar
Br = 0.45
½d spacing

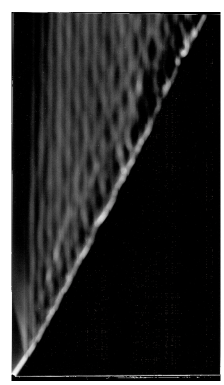

Fig 4e,
75%Ar
Br = 0.45
½d spacing

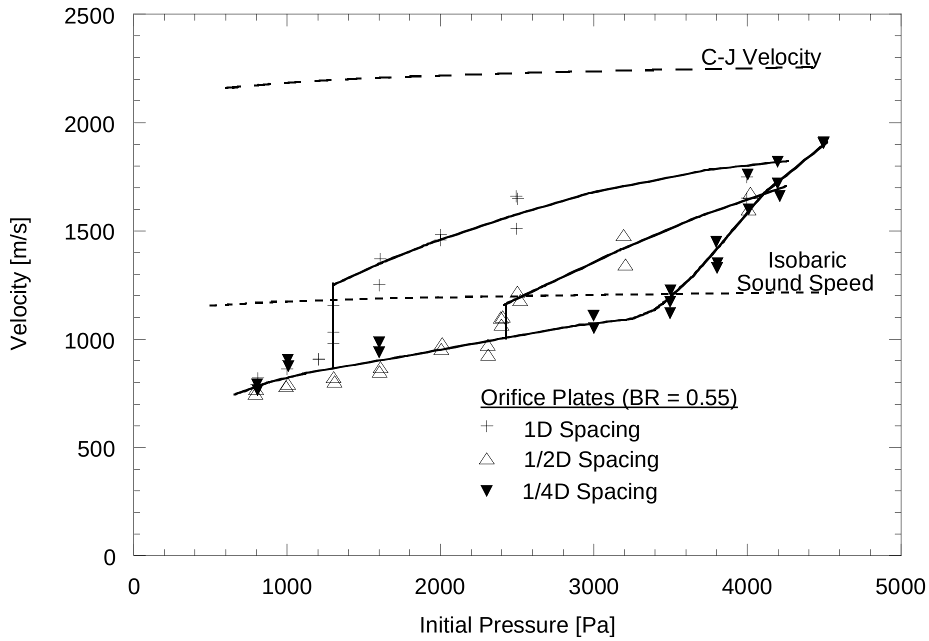

Figure 5: Effect of Spacing on Transition Location

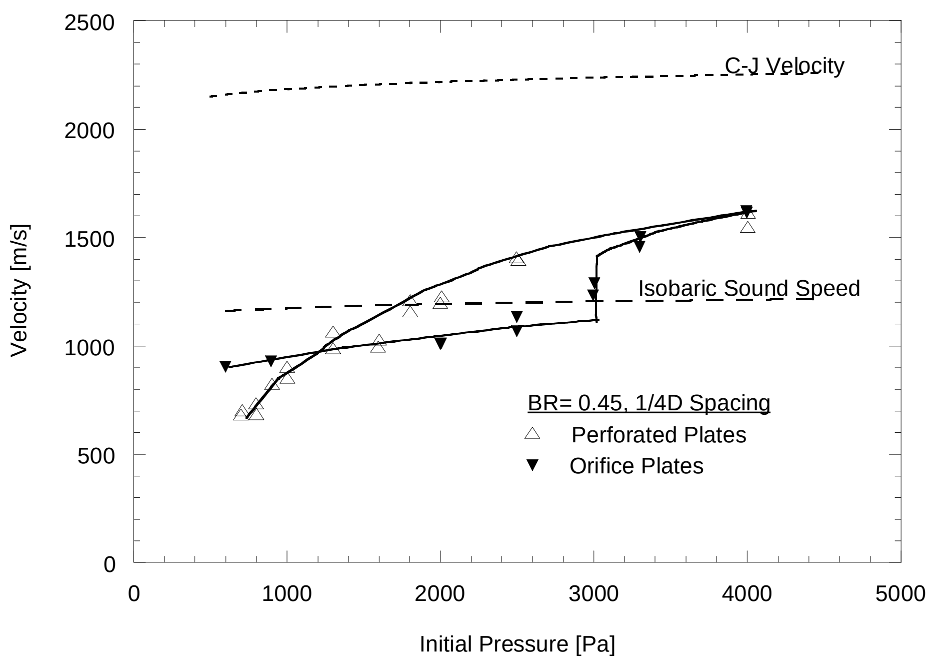

Figure 6: Effect of Obstacle Geometry on Transition Location